Electric and hydrodynamic stretching of DNA-polymer conjugates in free-solution electrophoresis

S. Nedelcu
Department of Physics, University of Ottawa, 150 Louis Pasteur, Ottawa, Ontario K1N 6N5, Canada

R. J. Meagher[a)]
Department of Chemical and Biological Engineering, Northwestern University, Evanston, Illinois 60208-3120

A. E. Barron
Department of Chemical and Biological Engineering, Northwestern University, Evanston, Illinois 60208-3120 and Department of Chemistry, Northwestern University, Evanston, Illinois 60208-3120

G. W. Slater
Department of Physics, University of Ottawa, 150 Louis Pasteur, Ottawa, Ontario K1N 6N5, Canada

(Received 5 October 2006; accepted 22 March 2007; published online 7 May 2007)

The conjugation of an uncharged polymer to DNA fragments makes it possible to separate DNA by free-solution electrophoresis. This end-labeled free-solution electrophoresis method has been shown to successfully separate ssDNA with single monomer resolution up to about 110 bases. It is the aim of this paper to investigate in more detail the coupled hydrodynamic and electrophoretic deformation of the ssDNA-label conjugate at fields below 400 V/cm. Our model is an extension of the theoretical approach originally developed by Stigter and Bustamante [Biophys. J. **75**, 1197 (1998)] to investigate the problems of a tethered chain stretching in a hydrodynamic flow and of the electrophoretic stretch of a tethered polyelectrolyte. These two separate models are now used together since the charged DNA is "tethered" to the uncharged polymer (and vice versa), and the resulting self-consistent model is used to predict the deformation and the electrophoretic velocity for the hybrid molecule. Our theoretical and experimental results are in good qualitative agreement.
 [DOI: 10.1063/1.2730799]

I. INTRODUCTION

The first method aimed at improving classical electrophoretic ssDNA sequencing methods used field-inversion polyacrylamide gel electrophoresis[1] and end-labeled ssDNA. Unfortunately, this new concept for separating nucleic acids by gel electrophoresis (which was called trapping electrophoresis) was eventually shown to be limited by catastrophic band broadening.[2] Similar end-labeled ssDNA molecules were later separated in free-solution electrophoresis;[3] this method is called ELFSE (which stands for end-labeled free-solution electrophoresis[4]). The label destroys the free-draining nature of DNA, a property that does not allow free-solution electrophoretic separations to be achieved.[5] The charge density along the hybrid molecule being nonuniform, it is possible to achieve separation without sieving by controlling this charge asymmetry (the resulting electrophoretic mobility becomes molecular size dependent).[6,7] The hydrodynamic interactions play a central role in our theory since the uncharged label attached to the DNA provides the only resistive frictional force that makes the free-solution separation possible. Recent advances in ELFSE label (or drag-tag) design, which focus on the development of polymeric labels, are slowly pushing the current maximum ssDNA sequencing read length beyond the value of 110 bases reported in 1999.[3]

This paper has two aims. First, we present the theoretical approach to study the complex electric and hydrodynamic interactions involved in the electrophoretic migration of the conjugate comprising the DNA and the neutral label. Then we investigate the conjugate's electrophoretic motion in the low field regime, both theoretically and experimentally. The theoretical approach we use is an extension of earlier work by Stigter and Bustamante.[8–11] The end-labeled ssDNA conjugate is seen as a continuous polymer chain made of a series of segments (charged in the case of DNA but uncharged in the case of the label) with different diameters and lengths (corresponding to those of the DNA and the label). A schematic depiction of our physical model is shown in Fig. 1. Each segment represents one Kuhn length each, while their diameter is related to the chemical nature of the monomers. In our model the charged ssDNA molecule is "tethered" to the uncharged polymer label, and both share the same finite velocity in the solvent.

Before we detail the plan of the article we mention here briefly a few reports on the free-solution electrophoresis of DNA, a problem which has been studied for several decades, both experimentally and theoretically.[12] Qualitatively, the result is only weakly dependent on the choice of the buffer for a typical ionic strength. Above a certain molecular weight, all DNA molecules then show the same mobility. The traditional reason given for this behavior involves the fact that both the driving force and the friction coefficient scale lin-

[a)]Present address: Sandia National Laboratories, Livermore, CA.

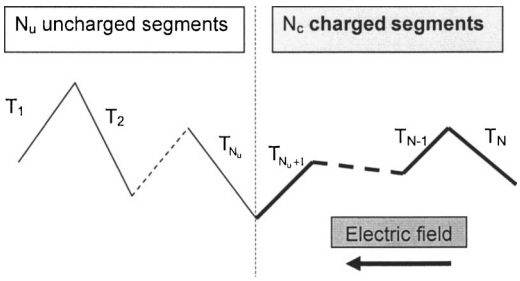

FIG. 1. Schematic drawing of the polymer model, with N_u uncharged and $N_c=N-N_u$ charged segments. The charged and uncharged segments may not be of equal lengths. The T_i is the tension on the ith segment. The attachment of the neutral polymer to the otherwise free-draining charged polymer is key to electrophoretic separation.

early with the molecular size in this limit.[13] Because of the linear increase of the electrophoretic friction coefficient with the DNA size, it is common to refer to DNA as a free-draining coil.

Long *et al.* studied the electrophoretic mobility of uniformly charged chains and periodically charged chains.[14–17] They showed that for dilute solutions of polyelectrolytes with no salt (an atypical experimental condition) the electric and hydrodynamic forces do not balance locally, which results in a buildup of tension and deformation of the coils in free-flow electrophoresis. At the opposite end, in a solution of high salt concentration Long *et al.* showed that the electric and hydrodynamic forces balance locally, which means that a uniformly charged chain moves without deformation and the mobility is size independent:[16] the coil is essentially in free fall under the action of the external electric field.

Volkel and Noolandi[13,18] used a Rotne-Prager tensor[19] to approximate the hydrodynamic interactions between monomers. Their analytic calculations of the free-solution electrophoretic mobility μ_0 of polyelectrolytes (in particular, ssDNA) predicted that μ_0 should increase with molecular size for short molecules (less than 20 bases for ssDNA) before saturation sets in.

An analytical expression for the free-solution electrophoretic mobility of a rodlike charged polyion has been obtained by Mohanty and Stellwagen.[20] Their approach took into account relaxation field effects, the screening of the velocity field, and the Oseen tensor for the hydrodynamic interactions. For oligomeric dsDNA they showed that the free-solution electrophoretic mobility increases with molecular weight up to a few hundred base pairs and noted that the free-solution mobility of ssDNA is smaller than that of dsDNA fragments of the same length at any given ionic strength.

Hoagland *et al.* determined experimentally the free-solution mobility of ssDNA for a wide range of ionic strengths.[21] They showed that μ_0 reaches a maximum value between 5 and 25 bases, then decreases slightly to a saturation value for longer chains. The same trend in the mobilities of ssDNA fragments has been observed by Stellwagen *et al.*; the reported value of the plateau mobility was 2.84×10^{-4} cm^2/V s in a 40 mM trisacetate buffer at 20 °C.[22] A gradual onset of coiling with an increase in molecular weight had been assumed to be responsible for the observed decrease in the mobility. It was argued that the interior of a coil is permeable to the solvent and therefore the counterions in the interior of the coil would migrate in the opposite direction to the negatively charged DNA molecules. This gradual increase in the drag force and/or the deformation of the polyion could be responsible for the variation of the mobility with molecular weight for short chains. The variation is, however, too small to be useful for separation purposes. We note that for the particular case of "no salt," Muthukumar predicted a weak dependence (proportional to $[\log(M)-1]$) for the free-solution mobility of a polyelectrolyte with M monomers.[23] The fractal dimension of the chain has been assumed to be unity and the polymer's shape to be rodlike because of the absence of salt.

In general, the exact solution to the electrophoretic migration of polymers requires that the Navier-Stokes, the Poisson, and the ion-transport equations are solved simultaneously.[24] This makes the problem very difficult and, if the perturbing fields are weak, the equations are usually linearized to simplify the problem. Allison and Stigter pointed out that for polyions which are not weakly charged (like dsDNA or ssDNA where $|e\zeta/k_BT|\approx3$, with ς the surface potential) a linear Poisson-Boltzmann equation may not provide valid transport properties.[25]

The plan of the article is as follows. In Sec. II we give a brief description of the polymer model of the ssDNA-label conjugate. We then examine the current ELFSE theories in Sec. III. The new experimental data on which we base our modeling are sequencing experiments employing a linear protein polymer drag tag[26] attached to ssDNA. The experimental method we use to analyze the data is not new and has been described in our earlier papers on ELFSE.[6] Note that a detailed description of the genetically engineered polymer label is going to be provided in an upcoming publication. The experimental part of the current paper thus focuses on explaining how we can determine the value of the parameters of our model from a fit of these new experimental data (Sec. IV). In Sec. V we discuss the overall chain extension along the field direction while the physical segregation between the ssDNA and the label is discussed in Sec. VI. We present our conclusions in Sec. VII and emphasize those aspects of our results which are in line with previous results based on scaling models or more explicit models, and what new insights into the electrophoretic motion of the end-labeled ssDNA are revealed by the present investigation. Also we comment briefly on aspects related to the range of use of scaling theories.

II. THE POLYMER MODEL FOR THE DNA-LABEL CONJUGATE

In this problem (see Fig. 1), we have two polymers linked together, one charged (the DNA) and one uncharged (the label). We consider worm-like chain semiflexible polymers, and we take into account the excluded volume interactions.

To find the electrophoretic mobility of the conjugate we start from earlier solutions by Stigter and Bustamante[8] to two separate problems: (1) a tethered uncharged polymer

stretched in a fluid flow and (2) a tethered polyelectrolyte stretched in an applied electric field. The original models are relatively simple: the DNA chain is modeled as a sequence of Kuhn segments joined together and subject to electric and hydrodynamic forces. For the electrical part of the total force acting on each Kuhn segment previous results on the electrophoretic velocity of an isolated cylindrical chain segment are used. The orientation of the segment relative to the applied field direction is explicitly taken into account, as well as the fact that the relaxation of the ionic atmosphere around the segment is zero if the segment is orientated parallel with the field and nonzero for perpendicular orientation. This is due to the asymmetry of the ionic atmosphere. The backflow of the ionic atmosphere is accounted for in both parallel and perpendicular orientations. The electric force depends also on the effective electrical charge of the segment, which is to say it depends on the electric surface potential. On the other hand, the hydrodynamic force acting on the segment is simply obtained by a superposition of hydrodynamic forces due to the neighboring segments. These segments were considered to be cylindrical in shape for the purpose of electrical solution of the problem; however, the analytical expressions for the hydrodynamics of short cylinders are not available; hence these cylindrical segments are converted into equivalent spheres of the same friction coefficient. Closed forms of the liquid velocity around ellipsoidal segments are then used.

In our present approach we use the same assumptions as in the original formulation: (1) the length of each polymer segment is the relevant Kuhn length (for either the DNA or the polymeric label); (2) the chain extension of each segment is given by the inverse Marko-Siggia[27] force-extension relation; (3) as far as hydrodynamic friction is concerned, each segment is thought of as a sphere with the proper Stokes friction (which is a long-range approximation of the flow pattern around the segment); (4) the relaxation of the ionic atmosphere and the perturbation of the local electric field are accounted for by a constant factor in the electrophoretic force on each segment; and (5) we neglect the effect of the electric forces on the friction coefficient of DNA segments and assume that Einstein's relation $f=k_BT/D$ between the friction coefficient f and the diffusion coefficient D remains locally valid (i.e., we neglect the fact that the relaxation of the ionic atmosphere may increase f slightly).

Let u_i be the velocity of the ith segment. As explained above the electric force acting on a segment is proportional to its surface potential (through the Smoluchowski equation for the electrophoretic effect) and additionally depends on its relative orientation to the applied field direction. It is the sum of the parallel $((\varepsilon_0\varepsilon\zeta E/\eta)f_{\parallel}^{(c)}\cos^2\theta_i)$ and perpendicular components $(\varepsilon_0\varepsilon\zeta E/\eta((2/3)g_{\perp})f_{\perp}^{(c)}\sin^2\theta_i)$, where the factor $(2/3)g_{\perp}$ accounts for the relaxation effect in the perpendicular orientation. In fact, as has been noted by Stigter this factor means that the local field on a segment orientated perpendicular to the field is smaller than the local field on the same segment if it were oriented parallel to the applied field. We can therefore write the final expression of the electrical force (which does not yet include the hydrodynamic interactions) acting on a single segment as follows:

$$F_i = \frac{\varepsilon_0\varepsilon\zeta E}{\eta}\left[f_{\parallel}^{(c)}\cos^2\theta_i + \frac{2}{3}g_{\perp}f_{\perp}^{(c)}\sin^2\theta_i\right], \tag{1}$$

where ε_0 is the permittivity of free space, ε is the buffer's dielectric constant, ζ is the surface potential of the DNA, η is the viscosity of the liquid, E is the applied electric field, and $g_{\perp}$ is a numerical factor.[8] The constant parameters $f_{\parallel}^{(c)}$ and $f_{\perp}^{(c)}$ are friction coefficients known in closed form for flow parallel and perpendicular to the long axis of a charged chain segment of ellipsoidal shape [note that the (c) in the superscript index indicates charged section and (u) will be used for the uncharged section]. As defined in Eqs. (6) and (7) of Ref. 8, the latter are functions of the aspect ratio $\phi^{(c)}=2p^{(c)}/c^{(c)}$ of the charged segment, where $p^{(c)}$ and $c^{(c)}$ are the persistence length (half of the long axis) and the length of the short axis of the Kuhn segment, respectively.

Similar to the problem of the hydrodynamic stretch solved earlier,[8] we consider the velocity of the uncharged segments as the sum of the electrophoretic velocity V_0 of the segment connecting the charged and uncharged sections of the hybrid molecule, plus the perturbation due to all the other segments (charged and uncharged):

$$u_i^{(u)} = V_0 + \sum_{j=1}^{N_u}\Delta u_{ij}^{(u)} + \sum_{j=N_u+1}^{N}\Delta u_{ij}^{(c)}, \quad i\neq j, \tag{2}$$

where $N=N_u+N_c$ is the total number of segments, and the perturbation term is given by Eq. (10) in Ref. 8:

$$\begin{aligned}\Delta u_{ij}^{(u,c)} &= \frac{u_j}{4}\left(-\frac{3a_j^{(u,c)}}{r_{ij}} - \frac{(a_j^{(u,c)})^3}{r_{ij}^3}\right) \\ &\quad + \frac{u_j}{4}\cos^2\theta_{ij}\left(-\frac{3a_j^{(u,c)}}{r_{ij}} + \frac{3(a_j^{(u,c)})^3}{r_{ij}^3}\right) \\ &\equiv u_j\xi_{i,j}^{(u,c)},\end{aligned} \tag{3}$$

where $\xi_{i,j}^{(u)}$ or $\xi_{i,j}^{(c)}$ are terms that depend on the orientation of the jth segment and the distance r_{ij} to the ith segment, and a_j is the radius of the equivalent sphere [Eq. (9) in Ref. 8]:

$$6\pi\eta a_j^{(u,c)} = f_{\parallel}^{(u,c)}\cos^2\theta_j + g_{\perp}f_{\perp}^{(u,c)}\sin^2\theta_j. \tag{4}$$

Using the notations in Eq. (3), the total electric [see Eq. (1)] and hydrodynamic forces that act on a single charged segment can now be written as

$$\begin{aligned}F_i^{(c)} &= \frac{\varepsilon\varepsilon_0\zeta E}{\eta}(f_{\parallel}^{(c)}\cos^2\theta_i + 2/3g_{\perp}f_{\perp}^{(c)}\sin^2\theta_i) \\ &\quad + 6\pi\eta a_i^{(c)}\sum_{j=1}^{N}{}'u_j\xi_{ij},\end{aligned} \tag{5a}$$

where the index i takes values from N_u+1 to N, and the prime sign in the sum means we neglect the term with $j=i$. Equation (5a) above is the same as Eq. (29) in Ref. 8. It can

be translated into segments' velocities according to the following expression:

$$u_i = \frac{\varepsilon\varepsilon_0\zeta E}{\eta}\left(\frac{f_{\parallel}^{(c)}\cos^2\theta_i + 2/3 g_{\perp} f_{\perp}^{(c)}\sin^2\theta_i}{f_{\parallel}^{(c)}\cos^2\theta_i + g_{\perp} f_{\perp}^{(c)}\sin^2\theta_i}\right) + \sum_{j=1}^{N}{}' u_j \xi_{ij}, \quad (5b)$$

where the first term is the contribution from the electric field and the sum represents the hydrodynamic interaction with the other segments. A convenient representation of Eqs. (2) and (5b), which combines both the velocities of the uncharged and charged segments, is obtained using the following matrix representation:

$$\begin{pmatrix} 1 & -\xi_{1,2} & \cdots & -\xi_{1,N_u} & -\xi_{1,N_u+1} & \cdots & -\xi_{1,N-1} & -\xi_{1,N} \\ -\xi_{2,1} & 1 & \cdots & -\xi_{2,N_u} & -\xi_{2,N_u+1} & \cdots & -\xi_{2,N-1} & -\xi_{2,N} \\ \cdots & \cdots & \cdots & \cdots & \cdots & \cdots & \cdots & \cdots \\ -\xi_{N_u,1} & -\xi_{N_u,2} & \cdots & 1 & -\xi_{N_u,N_u+1} & \cdots & -\xi_{N_u,N-1} & -\xi_{N_u,N} \\ -\xi_{N_u+1,1} & -\xi_{N_u+1,2} & \cdots & -\xi_{N_u+1,N_u} & 1 & \cdots & -\xi_{N_u+1,N-1} & -\xi_{N_u+1,N} \\ \cdots & \cdots & \cdots & \cdots & \cdots & \cdots & \cdots & \cdots \\ -\xi_{N-1,1} & -\xi_{N-1,2} & \cdots & -\xi_{N-1,N_u} & -\xi_{N-1,N_u+1} & \cdots & 1 & -\xi_{N-1,N} \\ -\xi_{N,1} & -\xi_{N,2} & \cdots & -\xi_{N,N_u} & -\xi_{N,N_u+1} & \cdots & -\xi_{N,N-1} & 1 \end{pmatrix} \begin{pmatrix} u_1 \\ u_2 \\ \cdots \\ u_{N_u} \\ u_{N_u+1} \\ \cdots \\ u_{N-1} \\ u_N \end{pmatrix} = \begin{pmatrix} V_0 \\ V_0 \\ \cdots \\ V_0 \\ e'_{N_u+1} \\ \cdots \\ e'_{N-1} \\ e'_N \end{pmatrix} \quad (6a)$$

where

$$e'_i = \frac{\varepsilon_0\varepsilon\zeta E}{\eta}\left(\frac{f_{\parallel}^{(c)}\cos^2\theta_\iota + (2/3) g_{\perp} f_{\perp}^{(c)}\sin^2\theta_i}{f_{\parallel}^{(c)}\cos^2\theta_i + g_{\perp} f_{\perp}^{(c)}\sin^2\theta_i}\right). \quad (6b)$$

The matrix formulation is very convenient to use in both cases, whether the label is attached to the DNA or not. The flowchart describing the different steps involved in the calculations is shown in Fig. 2. The averages $\langle\cos\theta_i\rangle$ or $\langle\cos^2\theta_i\rangle$ are calculated using Eqs. (20, 21) in Ref. 8. Starting from a random conformation of the chain (as described by the random angles between the segments) and the chosen parameters (polymer lengths, electric field intensity, viscosity, etc.), the electric forces and the local tensions are calculated first for the charged segments and then the calculation proceeds by calculating the "flow velocity" V_0 in Eq. (2), or the link velocity (the link is the point where the two polymers are connected), which is the local velocity of the last charged segment. The link velocity is required in order to calculate the velocities of the uncharged segments, which are assumed to move with an overall velocity equal to the link velocity plus a perturbation velocity. Next the velocities, forces, and tensions for the remaining uncharged segments are calculated. We note that this recursive calculation is such that the tension on the first segment (which is a free end) of the charged section and the tension on the last segment of the uncharged section (also a free end) are both zero. We also note that the total effective electrophoretic force on the DNA-label conjugate, which includes both the electric and the hydrodynamic contributions, must be equal to the difference in tensions between the last charged segment and the first uncharged segment. In the classical situation of a tethered polymer, only the tension on the free end is zero while the tension on the tethered end gives the total tethering force (the "link" then has zero velocity).

Generally, the numerical convergence of the electrophoretic force is achieved quite rapidly for short chains but requires more iterations for longer chains. The iterations are stopped when the relative change in the total electrophoretic force is less than 10^{-5}. We note that while the angles θ_i between the segments and the direction of the applied field are adjusted after each iteration, so as to achieve the convergence of the electrophoretic force, the initial azimuthal angles (ϕ) remain unchanged. Therefore, in order to reduce the influence of a particular initial ϕ configuration, we repeat the procedure several times so we can obtain statistical values independent of the sequence of random numbers (random angles ϕ) used. On average we use a set of 5000 different initial configurations. For each set of random coordinates and bond angles we calculate two electrophoretic velocities: first for a fully charged polymer chain, which means a DNA molecule without any attached label, and second for a partially charged polymer that corresponds to the same DNA but with a polymeric label attached. We shall see in the next section that we need this ratio of electrophoretic velocities to compare the predictions of our model to the experimental data. As expected, the electrophoretic mobility of DNA molecules is molecular size independent (results will be shown in Fig. 6; note that this is the reason why we need the drag tag to achieve free-solution separation). The input parameters of our numerical model are the total number of segments N, the number of uncharged segments N_u, the persistence lengths of the charged $p^{(c)}$ and uncharged $p^{(u)}$ segments (one-half the Kuhn length), the surface potential ζ of the ssDNA, the two chain diameters [charged $d^{(c)}$ and

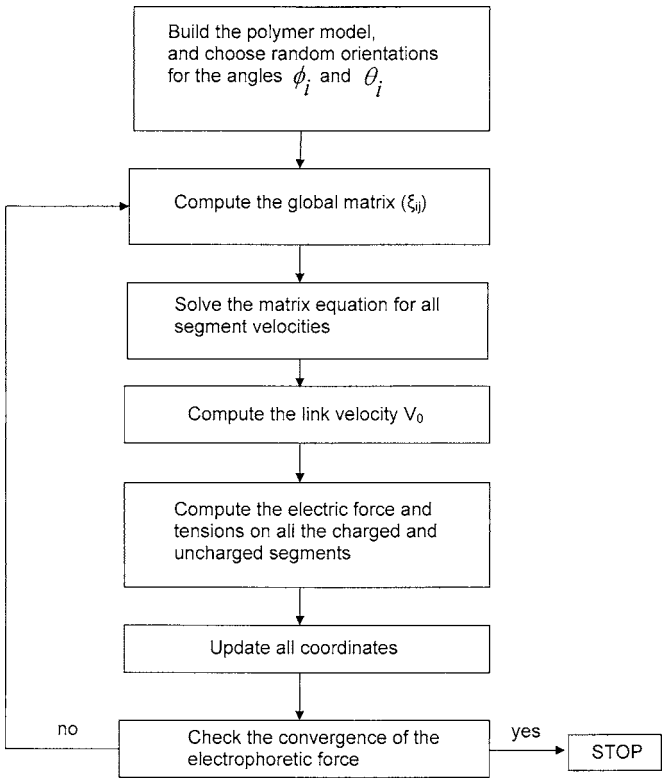

FIG. 2. Flowchart of the numerical calculations. Note the iterative nature of the calculation and the blending of the electric and the hydrodynamic velocity components, of either the charged or uncharged section of the chain, in a grand unifying matrix.

uncharged $d^{(u)}$], the dielectric constant or relative permittivity ε (=80) of the solution, the viscosity η (=1 cP) of the buffer, and the applied electric field E. We relate the short axis c of the ellipsoidal segment to the diameter d of a cylindrical chain segment via the relation $c^{(c,u)}=d^{(c,u)}\sqrt{1.5}$.[22] Except for the molecular weights of the two connected polymers, the dielectric constant, the viscosity of the solution, and the applied electric field, the fundamental molecular parameters of the model are unknown and must be found by fitting experimental data. In the following section, we review the fundamental ELFSE theory and explain how we obtain our model parameters, which are then used for the rest of the paper.

III. THE STANDARD ELFSE MOBILITY EQUATION

In order to explain the experimental ELFSE data, make predictions, and quantify the amount of hydrodynamic friction provided by the drag-tag label (which is a function of the monomer size, the polymer stiffness, the applied field, the buffer ionic strength, and possibly other parameters), an effective friction coefficient α has been defined by Mayer *et al.*[4] via the relation

$$\mu = \mu_0 \frac{M_c}{M_c + \alpha}, \tag{7}$$

where μ and μ_0 are the electrophoretic mobilities of the DNA-label conjugate and of the free DNA, respectively, and M_c is the number of charged monomers (bases of ssDNA in the case of sequencing). Since this relation can be rewritten as $\mu_0/\mu = 1+\alpha/M_c$, the experimental values of α have since been estimated using the slope of the linear fit that can be produced by plotting μ_0/μ vs $1/M_c$. In what was the first theoretical paper on ELFSE, Mayer *et al.* assumed that DNA remains free draining during ELFSE, and derive this relation in order to estimate the performance of this separation method. Although their predictions on the maximum read length of ELFSE were overestimated because of their use of the Nernst-Einstein relation (which is not always valid in electrophoresis),[28] we do note that their basic relation (7) has become the standard formula for analyzing all experimental work published to date. Three such notable examples are the papers of Heller *et al.*[29] on the separation of dsDNA by ELFSE, Ren *et al.*[3] on the sequencing of ssDNA, and the work of Sudor and Novotny[30] on the end-labeled, free-solution capillary electrophoresis (CE) of highly charged oligosaccharides; in all cases, the linear relation $\mu_0/\mu = 1+\alpha/M_c$ was found to be in good agreement with the experimental data.

The physical interpretation of the linear relation between μ_0/μ and $1/M_c$ varied, however, from the very first theoretical work in 1994 to the latest experimental investigation of ELFSE data.[26] Mayer *et al.* assumed in their calculations that the electrostatic and hydrodynamic interactions between the DNA and the friction generating label can be neglected, thus preserving the free-draining behavior of native DNA. On the other hand, Heller *et al.* suggested that the DNA fragments were almost entirely stretched during electrophoresis. After analyzing their experimental ELFSE data, Ren *et al.* concluded that the DNA-streptavidin complex does not deform during migration. The theoretical investigation of McCormick *et al.*[31] suggested that Eq. (7) remains valid as long as the charged and uncharged sections of the conjugate retain their Gaussian conformational statistics, i.e., as long as the two chains form a single random coil. In other words, Eq. (7) can only be valid in the low field intensity limit.

To account for the large difference in the persistence lengths of the DNA and of its polymeric label, a blob theory of ELFSE has been derived.[2] In essence, the blob theory regroups the charged and uncharged monomers into blobs of identical hydrodynamic properties. This construction then predicts that $\alpha=\alpha_1 M_u$ is the number of DNA monomers required to form a molecule with a hydrodynamic radius equal to the hydrodynamic radius of the coil formed by the M_u label monomers [the subscripts u and c refer to the uncharged (label) and charged (DNA) parts of the hybrid molecule, respectively]. The model also predicts that the new microscopic parameter α_1 can be written in terms of DNA and label properties as follows:

$$\alpha_l = \frac{b_u b_{Ku}}{b_c b_{Kc}}, \tag{8}$$

where b_x and $b_{Kx}=2p^{(x)}$ are the monomer size and Kuhn length of the polymer of type x. This relation agrees with the experimental data and provides evidence that the blob theory and Eq. (7) represent a good semimicroscopic theory of ELFSE.

The main quantities derived from our theory are the seg-

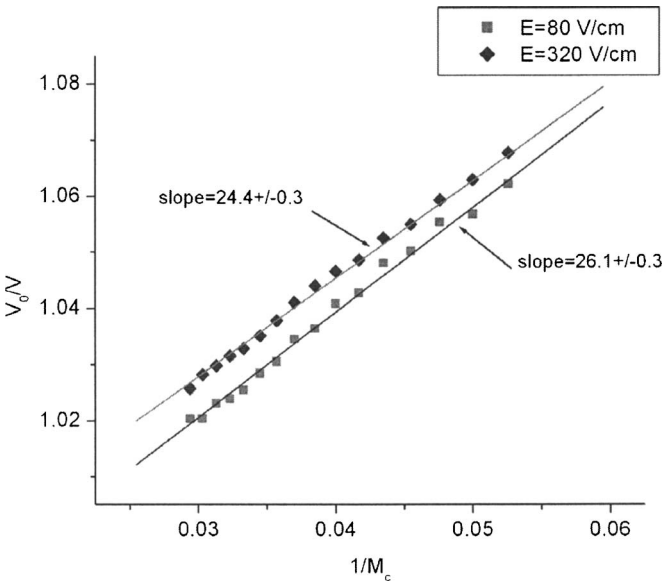

FIG. 3. Velocity ratio V_0/V vs the reciprocal number of charged monomers $1/M_c$ for two different values of the applied field E. The slope of the linear fit, which quantifies the friction provided by the neutral label, is $\alpha=\alpha_1 M_u$ [see Eq. (9)], where $M_u \equiv 127$. The model parameters are derived as explained in Sec. IV.

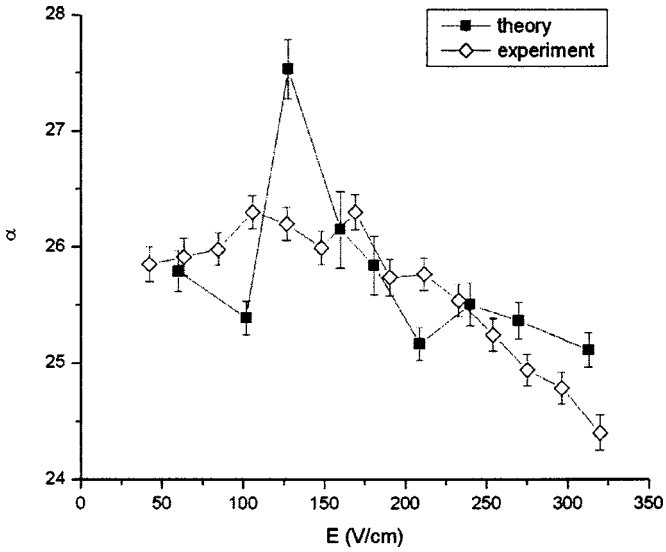

FIG. 4. Experimental and theoretical $\alpha(E)$ vs E curves. The theoretical fitting parameters are $p^{(c)}=3.0$ nm, $p^{(u)}=0.6$ nm, $d^{(u)}=0.9$ nm, $d^{(c)}=1.0$ nm, and $\zeta=0.0892$ V. The apparent decrease of $\alpha(E)$ at higher fields signals a lesser impact of the neutral label on the overall velocity of the conjugate.

ments' velocities. Accordingly, we rewrite Eq. (7) in terms of the electrophoretic velocities $V=\mu E$ and $V_0=\mu_0 E$:

$$\frac{V_0}{V} = 1 + \frac{\alpha_1 M_u}{M_c} \equiv 1 + \frac{\alpha}{M_c} \equiv 1 + \frac{\alpha'}{N_c}. \tag{9}$$

Since Eq. (7) appears to provide excellent fits for available experimental ELFSE data (note that all published data correspond to fields below 350 V/cm), the present theory must recover this fundamental empirical result. In Eq. (7) the α values calculated from the experiment are the slopes of the linear dependency of V_0/V to the reciprocal number of charged monomers $1/M_c$, and not to the reciprocal number of charged (Kuhn) segments $1/N_c$. The relation between α and α' simply follows from a definition of the total contour length of the charged polymer written as function of the number M_c of monomers or the corresponding number of Kuhn segments $M_c b^{(c)}=2N_c p^{(c)}$; therefore, $\alpha'=\alpha b^{(c)}/2p^{(c)}$, where $b^{(c)}=0.43$ nm is the monomer size of ssDNA. A similar relation allows us to make the connection between N_u and the actual size of the drag tag: $M_u b^{(u)}=2N_u p^{(u)}$. For simplicity we chose $b^{(u)}=b^{(c)}$.

Remarkably, the linear dependency between V_0/V and $1/M_c$ in Eq. (9) is also predicted by our numerical calculations (results are shown in Fig. 3 for two particular values of the applied field E) when the field is in the experimentally relevant range (the high field regime will be treated in a future article). The microscopic parameters used for this example correspond to the conditions used in our experimental study, as will be explained in the next section. This linearity is a central result of our theoretical calculation since no *a priori* assumption was made about the conformation of the DNA-label complex. Although the linear relation between V_0/V and $1/M_c$ may not be perfect for very small or very large DNA sizes,[32] we restrict ourselves to the linear regime since it is relevant for our experimental data. It is clear from the theoretical data in Fig. 4 that the effective friction coefficient α is predicted to be slightly field dependent; α first increases and then decreases slowly as the field increases further.

IV. COMPARISON OF THEORY WITH EXPERIMENT

Data for the electric field dependence of α were collected from a series of ELFSE sequencing experiments employing a linear protein polymer drag tag,[26] which will be described in detail in an upcoming publication. Briefly, a single-base "ladder" of drag-tag-modified ssDNA products was created by performing a dye terminator sequencing reaction using a primer that was covalently modified at the 5′ end with a protein polymer drag-tag molecule. The drag tag, which was described previously for ELFSE separation of dsDNA,[32] had a total length of 127 amino acids, with the highly repetitive sequence $(GAGTGSA)_4$-GAGTGRA-$(GAGTGSA)_7$-GAGTGRA-$(GAGTGSA)_5$-G. The protein polymer was produced by genetic engineering of *E. Coli* using the controlled cloning method described previously.[33–35] Following isolation and purification, the protein polymer was activated at the *N* terminus with Sulfo-SMCC, yielding a maleimide-activated 127mer drag tag with a net charge of +1. The activated drag tag was then conjugated to a reduced, 5′-thiolated, 17-base M13 sequencing primer [5′-HS-GTTTTCCCAGTCACGAC], which was used to generate a short M13mp18 sequencing ladder using dichlororhodamine dye terminator chemistry.

Electrophoretic separations of the drag-tag-modified ssDNa sequencing ladder were performed in free solution using an Applied Biosystems Prism 3100 genetic analyzer. Separations were performed at 55 °C in fused-silica capillaries with an inner diameter of 50 μm and an effective length of 36 cm (total length of 47 cm). Separations were performed in a denaturing buffer consisting of 1X TTE (89 mM tris, 89 mM TAPS, and 2 mM EDTA) with 7*M* urea, with

TABLE I. Experimental α values for the G-, C-, T- and A-terminated ssDNA fragments. The last two columns give the mean values and the corresponding standard deviations.

E (V/cm)	G	C	T	A	α	$\pm$
60	24.92	24.54	⋯	24.55	24.67	0.18
102	26.21	25.84	26.11	25.96	26.03	0.14
128	28.35	27.72	27.86	27.73	27.91	0.26
160	27.05	26.4	27.22	27.17	26.96	0.33
181	26.15	26.4	26.05	26.84	26.49	0.26
209	26.00	26.32	26.10	26.32	26.18	0.14
240	25.43	25.86	25.53	25.82	25.66	0.18
270	24.98	25.34	25.04	25.30	25.16	0.16
313	24.76	24.11	24.83	25.07	24.94	0.15

1% (v/v) of POP-6 solution added to the running buffer to suppress electro-osmotic flow (see, for example, the discussion in Ref. 3 on the dynamic wall coating agent). Samples were injected electrokinetically at approximately 22 V/cm for 20 s. The electric field used for separation varied from 60 to 310 V/cm.

The α value at each field strength was determined from the observed migration times of each size of ssDNA in the range $18<M_c<120$ bases, relative to the migration time of ssDNA with no drag tag. Since the linear fit of the data is almost perfect,[26] we used Eq. (7) for the fits and we neglect the effect of the small positive charge present on the drag tag.

The elution order of the fragments is from the shortest to the longest fragment, which is the opposite in classical CE experiments. Each fragment of a set size (G, C, T, or A terminated) corresponds to a peak on the electrophoreogram and thus the elution time is known. In order to calculate α we also need to know the size of these fragments. In ideal conditions and for a perfectly monodisperse label, and clearly defined, not overlapping, sharp peaks the size of the eluted fragments simply increases by 1 up from the size of the primer (17 ssDNA bases). In our experiments we also know beforehand the size of each fragment since we know the control DNA template and thus we can make corrections for the mobility shift due to the four different dyes. We obtain an almost perfect linear dependency between the inverse mobility ratio μ_0/μ and the inverse molecular size $1/N_c$, as predicted by Eq. (7). Table I gives the experimental α values for each G, C, T, and A-terminated fragments together with the mean values. We notice that variance in α is not insignificant, with a difference of about 0.45 between the G- and A-terminated fragments.

Finding the parameters ζ, $p^{(c)}$, $p^{(u)}$, $d^{(c)}$, and $d^{(u)}$ that are needed for our calculation to reproduce the experimental α values given in Table I requires in essence the minimization of a function of five variables. We fit the experimental $\alpha=\alpha(E)$ curves using the least squares method. The fitting procedure is as follows. First we choose the field intensity E and starting values for ζ, $p^{(c)}$, $p^{(u)}$, $d^{(c)}$ and $d^{(u)}$. Note that since we know M_u (the true molecular size of the drag tag, which does not change) and the current value of $p^{(u)}$, we can estimate N_u for the given iteration. We then vary the number of charged segments N_c such that we can calculate the α' value from the slope of the linear dependency at this particular field E [see Eq. (9)]. We repeat this procedure for other field intensities and we finally obtain one theoretical $\alpha=\alpha(E)$ curve. The next step is to calculate the deviation of the theoretical curve from the experimental data. Depending on the magnitude of the errors more iterations may be required until the errors are minimal. We restricted the range of values explored for the five parameters in order to only explore those parts of the parameter space that make sense experimentally. The agreement with the experimental data is fair (Fig. 4). The best fitting parameters were found to be $p^{(c)}=3.0$ nm, $p^{(u)}=0.6$ nm, $d^{(u)}=0.9$ nm, $d^{(c)}=1.0$ nm, and $\zeta=0.0892$ V. We note that our experimental data give $\alpha_1\equiv\alpha/M_u\approx 26/127\approx 0.205$, while the blob theory gives $\alpha_1=0.6/3.0=0.2$ if we use Eq. (8) and the fitting parameters above.

V. CHAIN EXTENSION ALONG THE FIELD DIRECTION

The extension (or deformation) of the charged and uncharged sections of the DNA-label complex along the direction of the field provides an excellent way to understand the response of the hybrid molecule to the applied field (Fig. 5). At the beginning of each calculation the chain is created in a state of random coil, with random positions and orientations for each segment. Depending on the value of the applied field, the chain can remain in this state or, if the applied field is high, the chain can stretch and eventually reach complete stretching. In the latter case the sum of segment projections Z_i (Fig. 5) must be equal to the contour length $M_c b^{(c)}+M_u b^{(u)}=2N_c p^{(c)}+2N_u p^{(u)}$ of the polymer.

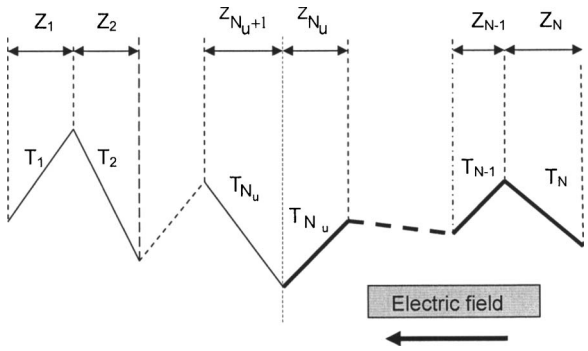

FIG. 5. Schematic of the projection of the polymer segments on the applied field direction that quantifies the chain extension.

We will quantify the response of the DNA-label conjugate to the electric field by calculating the mean extensions $e^{(c,u)}$ of the charged and uncharged segments:

$$e^{(c)} = \frac{1}{2p^{(c)}N_c}\left(\sum_{i=N_u+1}^{N} Z_i\right), \tag{10}$$

$$e^{(u)} = \frac{1}{2p^{(u)}N_u}\left(\sum_{i=1}^{N_u} Z_i\right), \tag{11}$$

where the values of the fitting parameters are those given in Sec. IV. Two important limits need to be mentioned about Eqs. (10) and (11). If the DNA and the label are in a state of random coil, the sums over segment projections must be zero. When the field is increased, the segments may align preferentially along the direction of the applied field, which would make the normalized extensions *increase* towards unity, the maximum normalized value of these projections.

In Fig. 6(a) we show these segmental orientations as a function of the applied field E for one particular label size (M_u=127 monomers, which corresponds to ≅45 Kuhn uncharged segments given the fitting parameters obtained previously). The total length N of the polymer model is varied, as would be the case for ssDNA sequencing by ELFSE. We chose N_c=18, N_c=26, and N_c=34. The persistence lengths of the uncharged and charged segments are $p^{(u)}$=0.6 nm and $p^{(c)}$=3.0 nm, respectively, and these values can be used to link the number of monomers to the number of Kuhn segments, as described in Sec. III. For instance, the $\{N_c=18; N_u\approx 45\}$ case corresponds to having 127 uncharged label monomers attached to a 251 base long ssDNA molecule.

As Fig. 6(a) demonstrates, labeled DNA orients more than free DNA. In both cases, however, the degree of orientation is rather small. One can measure the importance of this orientation by comparing the scaled random-walk end-to-end distance $h_{\mathrm{RW}}\sim\sqrt{N_c}$ with the component coming from orientation, $h_E\sim N_c\langle e^{(c)}\rangle$. Using the midvalues N_c=26 and $\langle e^{(c)}\rangle$ =0.1, we obtain $h_{\mathrm{RW}}\cong 5$ and $h_E\cong 2.6$, showing that the DNA chains are only weakly deformed. Figure 6(b) also shows that the label itself stretches only moderately and that the amount of stretching is a rather weak function of the size of the DNA. Here, a simple calculation gives the rough values $h_{\mathrm{RW}}\sim\sqrt{N_u}\cong 7$ and $h_E\sim N_u\langle e^{(u)}\rangle\cong 1$. The small degree of orientation we see in Fig. 6(a) for free, short ssDNA has not been reported before, but it would be quite hard to observe in practice. (For double-stranded DNA we mention here the work of Jonsson *et al.*[36] that measured for T2 DNA an extension of the coil by roughly a factor of 3 during free-solution electrophoresis.) We note that DNA orients substantially more than the label: this is a direct consequence of the fact that it is more difficult to stretch more flexible polymers before they have more conformational entropy (the label is about five times more flexible than the DNA here).

Figure 6(c) clearly shows that the mobility of free DNA is predicted to be field independent, which agrees with experimental results. For a quantitative comparison, the free-solution mobilities of short ssDNA fragments, measured at low fields ($E<350$ V/cm), are shown in Fig. 6(d). The sizes

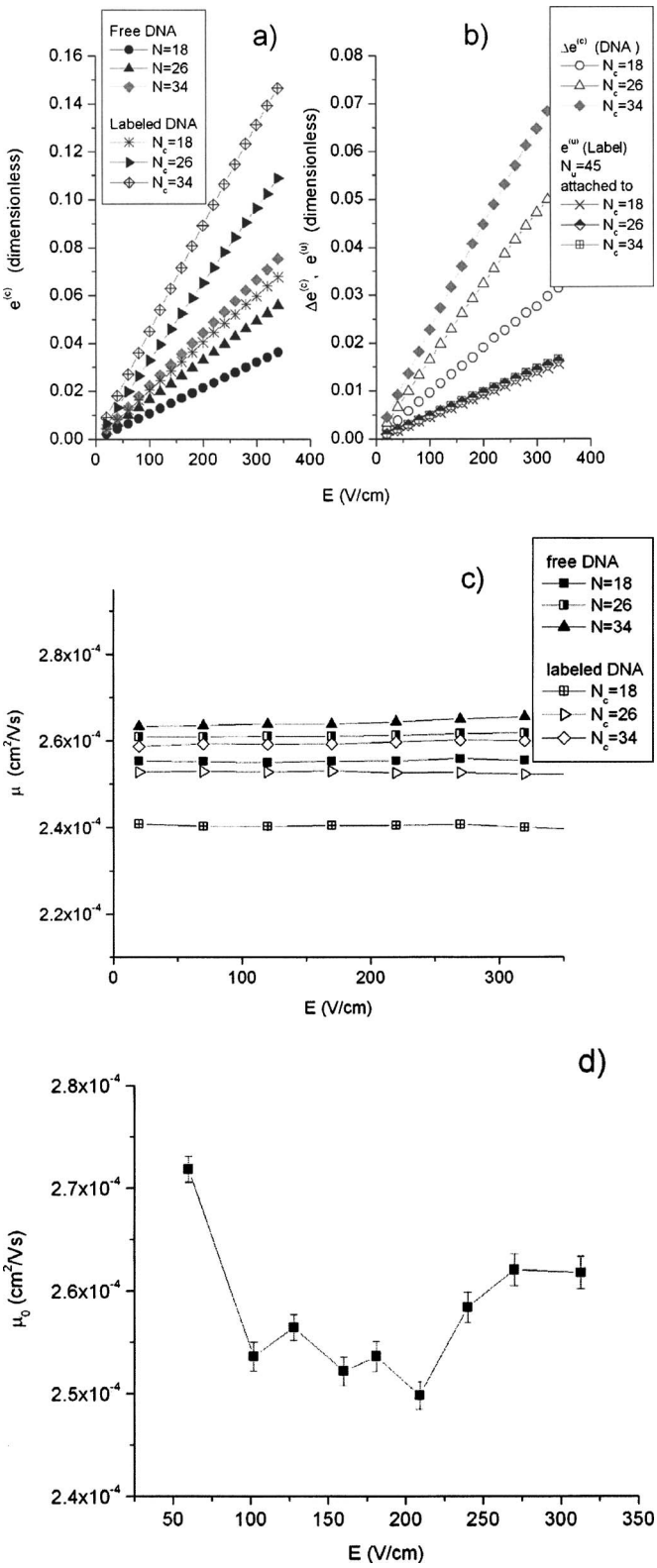

FIG. 6. A quantitative estimation of the conjugate extension in response to the applied field. (a) Total normalized extension per segment $e^{(c)}$ for free and labeled DNA and (b) extension $e^{(u)}$ for the label and the additional extension $\Delta e^{(c)}=e^{(c)}_{\text{labeled DNA}}-e^{(c)}_{\text{free DNA}}$ of the DNA due to the label vs the applied electric field intensity E for three different DNA sizes N_c=18, N_c=26, and N_c =34 and a label of size M_u=127 (or N_u=45). (c) The predicted free-solution mobility of DNA and the mobility of the DNA-label conjugate as function of applied field. (d) Experimental values of the average free-solution mobility of ssDNA with sizes between 18 and 160 bases at fields below 350 V/cm. The error bars correspond to the width of the Gaussian peaks at half height and are representative only of a single run experiment.

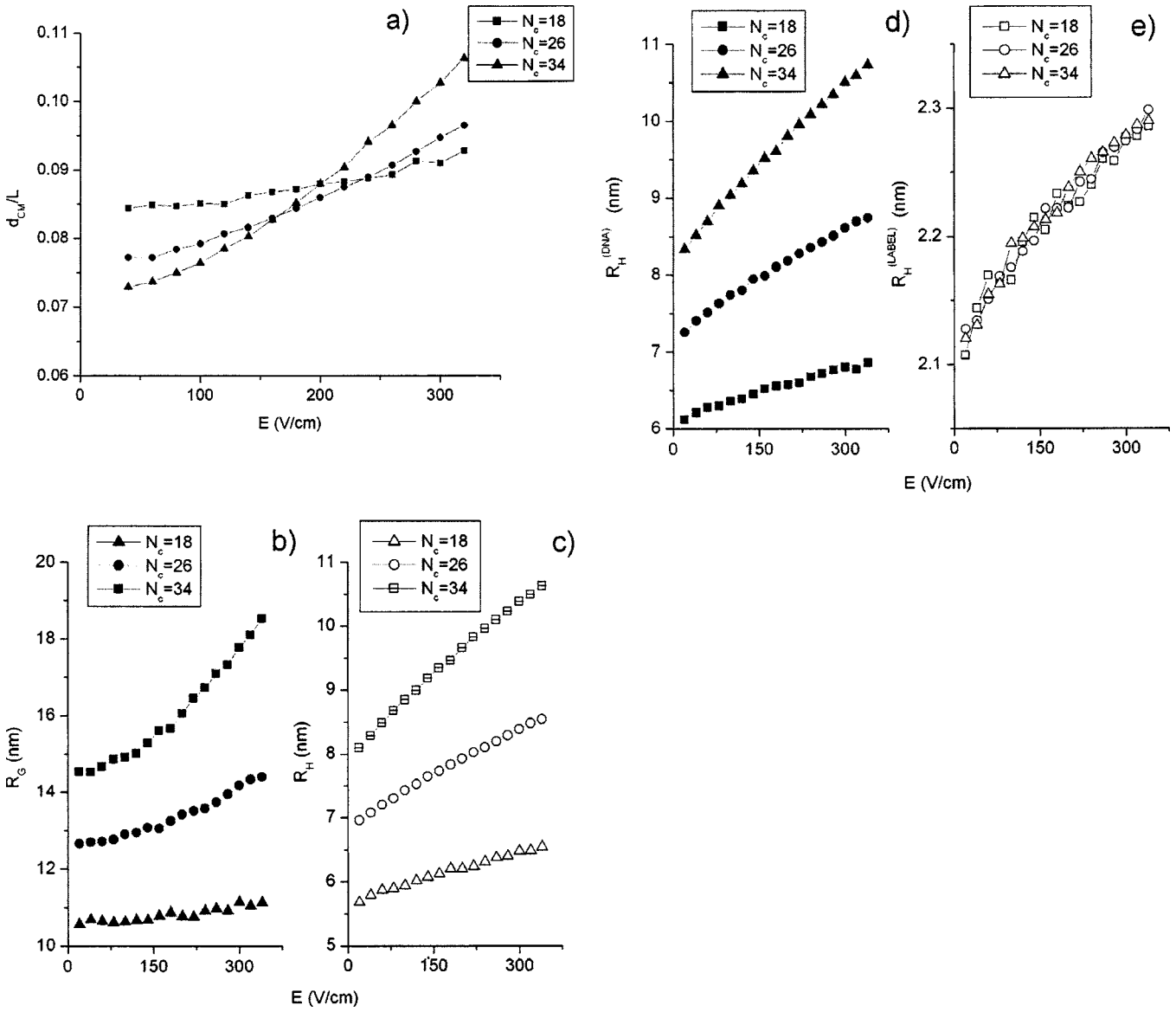

FIG. 7. Quantifying the ssDNA-label segregation and size effects for a fixed-length label. (a) The dimensionless ratio of the distance $d_{\text{c.m.}}$ between the center of mass of the DNA and the label over the total contour length $L=N_c 2p^{(c)}+N_u 2p^{(u)}$ of the conjugate, (b) the gyration R_G and (c) total hydrodynamic R_H radius of the conjugate for three different lengths N of the complex and a fixed length $M_u=127$ of the label, and (d) individual hydrodynamic radii of the DNA $R_H^{(\text{DNA})}$ and (e) the label $R_H^{(\text{label})}$. Because of entropic effects, not surprisingly, larger ssDNA chains appear to be more easily deformed.

of the ssDNA fragments are between 18 and 160 bases and they appear on the electrophoreogram as a single wide Gaussian peak, which presumably come from the overlapping of indistinguishable separate sharp peaks corresponding to each fragment. The width of the Gaussian distributions is indicative that the free-solution mobility of ssDNA is so slightly dependent on the ssDNA size. The plotted experimental free mobilities in Fig. 6(d) are, in fact, the maxima of these Gaussian peaks for each experiment. Our numerical values agree with the experimental data.

VI. SEGREGATION AT LOW FIELDS

In previous ELFSE theories[6] it has been assumed that during electrophoresis the DNA-label conjugate can adopt different conformations (see Fig. 2 in Ref. 5): random coil (a logical assumption in the low field limit), "dumbbell" conformations where there is physical and hydrodynamic separation between the undisturbed label and the undisturbed DNA molecule, or conformations where either or both components are stretched by the drag forces. It was predicted that this latter case would be met at very high fields (several kV/cm), much higher than the values usually reached in standard capillary electrophoresis experiments (about 300 V/cm).

One way to characterize the chain degree of segregation and deformation is to calculate the mean scalar distance $d_{\text{c.m.}}=\sqrt{(\mathbf{R}_{\text{DNA}}-\mathbf{R}_{\text{label}})^2}$ between the mass centers of the charged and uncharged sections as function of the applied field E, where $\mathbf{R}_{\text{DNA}}$ and $\mathbf{R}_{\text{label}}$ are the positions of the centers of mass for the DNA and label, respectively. This distance is a function of the contour lengths of the two sections. In the case where both polymers are relatively short, it is reasonable to assume that the DNA and the label might actually segregate for purely steric reasons (i.e., even at zero field),

while for longer chain lengths it might be assumed that the complex is in a global state of random coil at low fields and completely segregated at higher fields. Figure 7(a) shows the ratio of $d_{\text{c.m.}}$ to the total contour length of the conjugate, $L_c = N_c 2p^{(c)} + N_u 2p^{(u)}$, for the three DNA sizes ($N_c=18$, $N_c=26$, and $N_c=34$) studied in the previous section. The maximum value is a ratio of $\frac{1}{2}$. We note from Fig. 7(a) that $d_{\text{c.m.}}$ is not zero at low field; this is expected since the two centers of mass cannot be superimposed. As the field is increased, the segregation distance $d_{\text{c.m.}}$ increases gradually, and this separation is larger for the larger DNA molecule.

The radius of gyration and the hydrodynamic radius of the hybrid polymers are shown in Figs. 7(b) and 7(c), respectively. In both cases the net geometric size of the molecule increases gradually. However, if we look at the hydrodynamic radii of the two components separately [Figs. 7(d) and 7(e)], we observe a very weak deformation of the label which is almost independent of the DNA size; this is due to the fact that the deformation of the label is entirely due to the velocity of the molecule, which is a rather weak function of N_c here.

The zero-field data in Fig. 7(d) give $R_{h,0}^{\text{DNA}} \sim N_c^{1/2}$, showing that the excluded volume interactions are not important for these molecular sizes. Since the hydrodynamic radius of the label is much smaller than that of the DNA, we can write that $R_{h,0} \cong R_{h,0}^{\text{DNA}}$ [compare Figs. 7(c) and 7(d)] and similarly for the equilibrium radii of gyration. Polymer deformation should occur when the applied forces exceed the entropic forces that are trying to restore the random coil conformation. Therefore, the critical electric field for segregation should satisfy the approximate relation

$$v(E) 6\pi\eta R_{h,0} \approx \frac{k_B T}{R_{G,0}}. \tag{12}$$

The left-hand side of this relation is a measure of the frictional forces on the undeformed molecule while the right-hand side is the entropic force. Using $v(E) \cong \mu_0 E$, this relation becomes

$$E^* \approx \frac{84}{R_{G,0}(\text{nm}) \times R_{h,0}(\text{nm})} \text{ kV/cm}. \tag{13}$$

We first notice that we predict $E^* \sim 1/N_c$ using this expression (since $R_{G,0}^{\text{DNA}} \sim R_{h,0}^{\text{DNA}} \sim N_c^{1/2}$). If we now consider the $N_c=34$ case, the equilibrium radius of gyration is $R_{g,0} \cong 15$ nm [Fig. 7(b)] while the hydrodynamic radius is $R_{h,0} \cong 8$ nm [Fig. 7(d)]. Equation (13) then predicts $E^* = 700$ V/cm, which is consistent with the fact that our results show small molecular segregation. Higher fields would be required to observe such effects. It is interesting to note that the small degree of molecular orientation and of segregation does not affect the validity of Eqs. (7)–(9), which may explain their success in describing previous experimental results.

To complement the discussion above, we show in Fig. 8 the effect of the electric and hydrodynamic forces on typical molecular conformations for two different conjugates and three different field intensities. A quick inspection of these illustrations seems to be in line with the quantitative discussion above. Moreover, it is apparent that the electrophoretic stretch is higher near the joining point of the DNA to the label, and relatively lower near the free end of the chains, which is in good agreement with results in Ref. 22, if we consider the uncharged label playing the role of the "tethering" force that opposes the movement of the charged DNA.

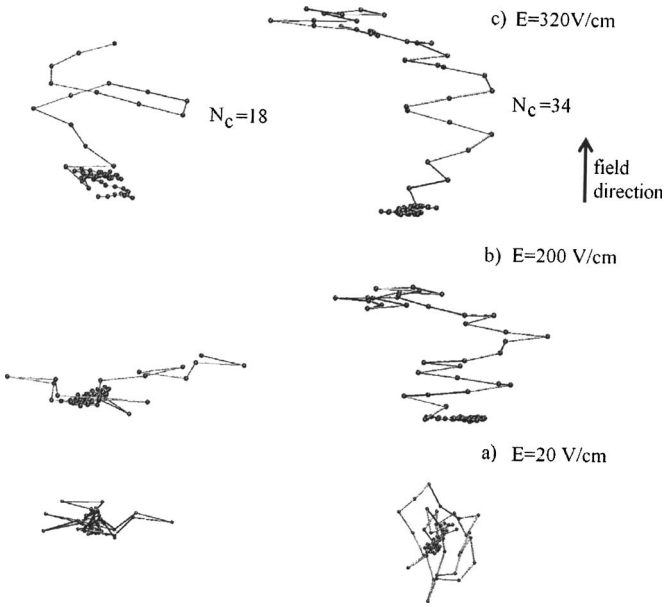

FIG. 8. Typical molecular conformations that show the gradual increase in the orientation of the chains as the field increases for two different conjugates with (left) $N_c=18$ and (right) $N_c=34$ charged segments attached to a set-length label $M_u=127$ (or $N_u \approx 45$) at three different applied fields: (a) $E=20$ V/cm, (b) $E=200$ V/cm, and (c) $E=320$ V/cm.

VII. CONCLUSION

We have developed a simulation model based on earlier work of Stigter and Bustamante[8] in order to calculate the free-solution electrophoretic mobility of ssDNA that has a neutral polymer label attached to it. Using new experimental data for low electric field intensities, we obtained fitting parameters (e.g., the persistence lengths of the neutral label and the ssDNA) that were in good agreement with the expected values. Using these fitting parameters and earlier ELFSE theories, in particular, the blob theory,[2] we obtained a good agreement as far as the total hydrodynamic friction provided by the label was concerned. There is, however, a departure from the scaling theories since the present investigation reveals a continuous disentanglement of the ssDNA from the label as the applied field increases from zero to its current value, with the final consequence that the hydrodynamic friction provided by the label becomes necessarily field dependent. This field dependency of the hydrodynamic friction is a new result and is confirmed by the experiment.

The DNA-label conjugate's response to the applied field has been investigated by corroborating various aspects of the dynamics: the variation with the field of the extension of the uncharged and charged sections of the conjugate, the segregation of the two submolecules, and the total hydrodynamic and gyration radii. We predicted that the DNA and the label are not strongly segregated or deformed at fields below 400 V/cm. In spite of a small degree of molecular orienta-

tion (which could not be studied with our previous scaling theories), the equations used in the past to fit experimental data were found to remain valid. However, we predicted (and observed) a weak field dependence of the effective friction coefficient α, an effect that was missed by previous theories.

The method presented in this paper is novel and provides a microscopic theory of ELFSE that can be used to make predictions in intermediate regimes where scaling arguments are difficult to use. In situations where there is a complete segregation of the ssDNA from the neutral label due to the high field, and at the same time, when the sizes of both the ssDNA and the label are sufficiently large, it is expected that scaling theories can be safely applied in predicting the behavior of the conjugate. In a future article we will explore the physics of ELFSE at fields exceeding 400 V/cm.

ACKNOWLEDGMENTS

This work has been supported by the U.S. National Institutes of Health (NIH) (Grant No. NHGRI R01HG002918-01) and Northwestern University. The authors would like to thank L. McCormick for interesting discussions. The High Performance Computing Virtual Laboratory (HPCVL), the Shared Hierarchical Academic Research Computing Network (SHARCNET), and Western Canada Research Grid (WESTGRID) are gratefully acknowledged.

[1] L. Ulanovsky, G. Drouin, and W. Gilbert, Nature (London) **343**, 190 (1990).
[2] C. Desruisseaux, D. Long, G. Drouin, and G. W. Slater, Macromolecules **34**, 44 (2001).
[3] H. Ren, A. E. Karger, F. Oaks, S. Menchen, G. W. Slater, and G. Drouin, Electrophoresis **20**, 2501 (1999).
[4] P. Mayer, G. W. Slater, and G. Drouin, Anal. Chem. **66**, 1777 (1994).
[5] B. M. Olivera, P. Baine, and N. Davidson, Biopolymers **2**, 245 (1964).
[6] R. J. Meagher, J. I. Won, L. C. McCormick, S. Nedelcu, M. M. Bertrand, J. L. Bertram, G. Drouin, A. E. Barron, and G. W. Slater, Electrophoresis **26**, 331 (2005).
[7] W. N. Vreeland, C. Desruisseaux, A. E. Karger, G. Drouin, G. W. Slater, and A. E. Barron, Anal. Chem. **73**, 1795 (2001).
[8] D. Stigter and C. Bustamante, Biophys. J. **75**, 1197 (1998).
[9] D. Stigter, J. Phys. Chem. **83**, 1670 (1979).
[10] D. Stigter, J. Phys. Chem. **82**, 1424 (1978).
[11] D. Stigter, J. Phys. Chem. **82**, 1417 (1978).
[12] J. L. Viovy, Rev. Mod. Phys. **72**, 813 (2000).
[13] A. R. Volkel and J. Noolandi, Macromolecules **28**, 8182 (1995).
[14] D. Long, J. L. Viovy, and A. Ajdari, J. Phys.: Condens. Matter **8**, 9471 (1996).
[15] D. Long, A. V. Dobrynin, M. Rubinstein, and A. Ajdari, J. Chem. Phys. **108**, 1234 (1998).
[16] D. Long, J. L. Viovy, and A. Ajdari, Phys. Rev. Lett. **76**, 3858 (1996).
[17] D. Long and A. Ajdari, Electrophoresis **17**, 1161 (1996).
[18] A. R. Volkel and J. Noolandi, J. Chem. Phys. **102**, 5506 (1995).
[19] J. Rotne and S. Prager, J. Chem. Phys. **50**, 4831 (1969).
[20] U. Mohanty and N. C. Stellwagen, Biochemistry **49**, 209 (1999).
[21] D. A. Hoagland, E. Arvanitidou, and C. Welch, Macromolecules **32**, 6180 (1999).
[22] E. Stellwagen, Y. Lu, and N. C. Stellwagen, Biopolymers **42**, 11745 (2003).
[23] M. Muthukumar, Electrophoresis **17**, 1167 (1996).
[24] S. A. Allison and S. Mazur, Biopolymers **46**, 359 (1998).
[25] S. A. Allison and D. Stigter, Biophys. J. **78**, 121 (2000).
[26] R. J. Meagher, Ph.D. thesis, Northwestern University, 2005.
[27] J. F. Marko and E. D. Siggia, Macromolecules **28**, 8759 (1995).
[28] B. Tinland, A. Pluen, J. Sturm, and G. Weill, Macromolecules **30**, 5763 (1997).
[29] C. Heller, G. W. Slater, P. Mayer, N. Dovichi, D. Pinto, J. L. Viovy, and G. Drouin, J. Chromatogr. A **806**, 113 (1998).
[30] J. Sudor and M. V. Novotny, Anal. Chem. **67**, 4205 (1995).
[31] L. C. McCormick, G. W. Slater, A. E. Krager, W. N. Vreeland, A. E. Barron, C. Desruisseaux, and G. Drouin, J. Chromatogr. A **924**, 43 (2001).
[32] R. J. Meagher, L. C. McCormick, R. D. Haynes, J. Won, J. Lin, G. W. Slater, and A. E. Barron, Electrophoresis **27**, 1702 (2006).
[33] J. I. Won, R. J. Meagher, and A. E. Barron, Electrophoresis **26**, 2138 (2005).
[34] J. I. Won and A. E. Barron, Macromolecules **35**, 8281 (2002).
[35] J. I. Won, R. J. Meagher, and A. E. Barron, Biomacromolecules **5**, 618 (2004).
[36] M. Jonsson, U. Jacobsson, M. Takahashi, and B. Norden, J. Chem. Soc., Faraday Trans. **89**, 2791 (1993).